Published in final edited form as:
Eur J Neurosci. 2009 December 3; 30(11): 2121–2133. doi:10.1111/j.1460-9568.2009.07005.x.

In Vivo Voltammetric Monitoring of Norepinephrine Release in the Rat Ventral Bed Nucleus of the Stria Terminalis and Anteroventral Thalamic Nucleus

Jinwoo Park, **Brian M. Kile**, and **R. Mark Wightman**
Department of Chemistry and Neuroscience Center, University of North Carolina at Chapel Hill, Chapel Hill, North Carolina 27599-3290, USA

Abstract

The role and contribution of the dense noradrenergic innervation in the ventral bed nucleus of the stria terminalis (*v*BNST) and anteroventral thalamic nucleus (AV) to biological function and animal behaviors is poorly understood due to the small size of these nuclei. The aim of this study was to compare norepinephrine release and uptake in the *v*BNST with that in the AV of anesthetized rats. Measurements were made *in vivo* with fast-scan cyclic voltammetry following electrical stimulation of noradrenergic projection pathways, either the dorsal noradrenergic bundle (DNB) or the ventral noradrenergic bundle (VNB). The substance detected was identified as norepinephrine based upon voltammetric, anatomical, neurochemical, and pharmacological evidence. Fast-scan cyclic voltammetry enables the selective monitoring of local norepinephrine overflow in the *v*BNST evoked by the stimulation of either the DNB or VNB while norepinephrine in the AV was only evoked by DNB stimulation. The α2-adrenoceptor antagonist, yohimbine, and the norepinephrine uptake inhibitor, desipramine, increased norepinephrine overflow and slowed its disappearance in both regions. However, control of extracellular norepinephrine by both autoreceptors and uptake was greater in the AV. The greater control exerted by autoreceptors and uptake in the AV resulted in reduced extracellular concentration compared to the *v*BNST when large numbers of stimulation pulses were employed. The differences in noradrenergic transmission observed in the terminal fields of the *v*BNST and the AV may differentially regulate activity in these two regions that both contain high densities of norepinephrine terminals.

Keywords

fast-scan cyclic voltammetry; norepinephrine uptake transporter; α2-adrenoceptor; dorsal and ventral noradrenergic bundle

Introduction

Norepinephrine is involved in the regulation of a number of behaviors including learning and memory, arousal and stress reactions to challenging environments, and drug addiction (Onaka & Yagi, 1998; Berridge & Waterhouse, 2003; Forray & Gysling, 2004; Aston-Jones & Cohen, 2005). Despite its important roles in the regulation of behavior, neuronal regulation of its release and uptake has been studied far less than for dopamine. In part, this is because the distribution of norepinephrine within the brain is diffuse (Mitchell *et al.*,

Corresponding Author: R. Mark Wightman, Ph.D., Department of Chemistry, Caudill Laboratories, University of North Carolina at Chapel Hill, Chapel Hill, NC, 27599-3290, USA, Tel : +1 (919) 962-1472, Fax : +1 (919) 962-2388, rmw@unc.edu.

1994) and high sensitivity is required for detection of its low physiological concentrations. Brain regions that have appreciable amounts of norepinephrine are often only a few hundred microns across (Kilts & Anderson, 1986; Palij & Stamford, 1992), further complicating detection.

Two important noradrenergic pathways in the brain are the dorsal noradrenergic bundle (DNB) and ventral noradrenergic bundle (VNB). The DNB primarily originates in the locus coeruleus (LC; A6) and then merges into the medial forebrain bundle with projections to targets that include the thalamus, hypothalamus, and cortex (Paxinos, 1995; Berridge & Waterhouse, 2003). The VNB has its origin in the nucleus tractus solitarius (NTS; A2) and other noradrenergic cell groups (A1, A5 and A7). It courses between the substantia nigra and ventral tegmental area (Ungerstedt, 1971; Johnston *et al.*, 1987) and then also merges with the medial forebrain bundle before projecting to target regions such as the septum and hypothalamus (Paxinos, 1995). Until they merge into the medial forebrain bundle, the VNB and DNB are distinct (Miyahara & Oomura, 1982; Saphier, 1993), facilitating independent excitation of each pathway by electrical stimulation. Electrically evoked norepinephrine can be detected with fast-scan cyclic voltammetry at carbon-fiber microelectrodes (Palij & Stamford, 1992), a technique demonstrated to be useful for monitoring the dynamics of extracellular dopamine in the brain (Millar *et al.*, 1985; Garris & Wightman, 1994; Owesson-White *et al.*, 2008). The high time resolution of this approach has enabled critical differences in the dynamics of extracellular dopamine to be characterized in specific brain regions such as the caudate-putamen and amygdala (Garris & Wightman, 1994). The small size (μm range) of the chemical sensor allows a local view of the dynamics of catecholamine release and uptake.

Here we report on norepinephrine release evoked by stimulation in the DNB and VNB. Release was monitored in the anteroventral thalamic nucleus (AV), a region characterized in previous work (Brun *et al.*, 1993; Dugast *et al.*, 2002) and compared to norepinephrine release in the ventral bed nucleus of the stria terminalis (*v*BNST), a region that receives a dense norepinephrine innervation (Oke *et al.*, 1983). The AV plays an important role in learning and memory while the *v*BNST regulates autonomic and behavioral responses related to stress, anxiety and noxious stimuli (Onaka & Yagi, 1998; Delfs *et al.*, 2000; Van Groen *et al.*, 2002). Comparison of noradrenergic transmission in the terminal fields in the *v*BNST and the AV provides new insights into the regulation of extracellular norepinephrine in these two regions that regulate very different aspects of animal behavior.

Materials and methods

Animals

Adult male Sprague-Dawley rats (320-400g) were purchased from Charles Rivers (Wilmington, MA) and housed in temperature and humidity controlled rooms with a 12 hour on/off light cycle. Food and water were available *ad libitum*. All procedures for handling and caring for the laboratory animals were in accordance with the Guide for Care and Use of Laboratory Animals and were approved by the Institutional Animal Care and Use Committee of the University of North Carolina at Chapel Hill.

Surgery

Male Sprague-Dawley rats were anesthetized with urethane (1.5 mg/kg) and immobilized in a stereotaxic frame (David Kopf Instruments, Tujunga, CA). Temperature was maintained at 37 °C with a heating pad (Harvard Apparatus, Holliston, MA). The dorsal skull surface was exposed, and small holes were drilled in the skull for reference (Ag/AgCl) and stimulating electrodes as well as the carbon-fiber microelectrodes. Anteroposterior (AP), mediolateral

(ML) and dorsoventral (DV) positions were referenced from bregma. The dura mater was punctured, carefully removed, and a carbon-fiber microelectrode was lowered into the BNST (AP 0.0 mm, ML +1.2 mm, DV from -6.0 to -8.0 mm), the AV (AP -2.1 mm, ML +1.5 mm, DV from -5.0 to -6.0 mm) or the CPu (AP +1.3 mm, ML +2.0 mm, DV from -4.5 to -6.5 mm; coordinates from a stereotaxic atlas (Paxinos & Watson, 2007). An Ag/AgCl reference electrode placed in the contralateral cortex was employed for all measurements and it was secured on the skull with dental cement.

Electrical stimulation was accomplished with a bipolar, stainless-steel electrode (0.2 mm diameter for each tip, the tips are separated by ~1.0 mm, Plastics One, Roanoke, VA). The stimulating electrode was insulated to the tip. It was placed into either the DNB (AP -5.2 mm, ML +1.2 mm, DV from -5.0 to -6.0 mm) or the VNB that is at the same AP and ML coordinates but is ~2 mm lower. Because the tips of the bipolar electrode were separated by ~1.0 mm, the VNB placement also stimulated the VTA and SN (Miyahara & Oomura, 1982; Saphier, 1993). Supplemental Figure 1 is a schematic of the ascending norepinephrine and dopamine pathways and the sites for their respective terminal areas (Ungerstedt, 1971).

Electrical stimulation

Stimulus pulses were computer-generated (NL 800A, Neurolog, Medical Systems Corp., Great Neck, NY, U.S.A.) and were electrically isolated from the electrochemical system. The electrical stimulation consisted of biphasic square wave pulses (300 μA and 2 ms each phase) with stimulation frequencies between 10 and 60 Hz. The number of stimulus pulses was normally held constant at 60 for the *v*BNST and the AV and 24 for the CPu. Stimulations were repeated every 4 or 5 min. With this time interval, stimulation resulted in reproducible responses for both norepinephrine and dopamine release. Shorter interval (< 2 min) resulted in diminished release.

Voltammetric procedures

Glass-encased cylindrical carbon-fiber microelectrodes and Ag/AgCl reference electrodes were prepared as described earlier (Cahill & Wightman, 1995). T-650 untreated carbon fibers (Thornel, Amoco Corp., Greenville, SC) with an exposed length of 75 - 100 μm and 6 μm in nominal diameter were used. fast-scan cyclic voltammetry was computer-controlled and has been described in detail previously (Heien *et al*., 2003). A triangular scan (-0.4 to +1.3 V, 400V/s) was repeated every 100 ms. Data was digitized and stored on a computer using software written in LABVIEW (National Instruments). Background-subtracted cyclic voltammograms were obtained by digitally subtracting voltammograms collected during stimulation from those collected during baseline recording. Temporal responses were determined by monitoring the current at the peak oxidation potential for norepinephrine and dopamine in successive voltammograms. The current was converted to concentration based on calibration curves of each carbon-fiber microelectrode obtained after the *in vivo* experiment with known concentrations of dopamine and norepinephrine *in vitro*.

High performance liquid chromatography (HPLC)

Rats were anesthetized with urethane and decapitated. The brain was rapidly removed and placed on ice. Coronal brain slices (500 μm thick) containing the ventral bed nucleus of the stria terminalis (*v*BNST) were prepared in ice cold artificial cerebral spinal fluid (aCSF) using a Lancer Vibratome (World Precision Instruments, Sarasota, Fl.). The aCSF contained (in mM): 20 HEPES, 2.4 $CaCl_2$, 1.2 $MgCl_2$, 1.2 NaH_2PO_4, 2.45 KCl, 126 NaCl, 11 glucose, and 25 $NaHCO_3$. The pH was adjusted to pH 7.4 and the aCSF was saturated with 95% O_2 / 5% CO_2. Tissue samples were dissected from the brain slices containing the area of interest (500 μm thickness). The tissue was wet weighted in a pre-tared volume of 200 μL 0.1 N $HClO_4$ spiked with 1 μM hydroquinone (HQ). The tissue was homogenized with a sonic

dismembrator (Fisher Sci., Model 60, Pittsburgh, PA, USA). The homogenized tissue was centrifuged at 6000 rpm for 10 min and the supernatant was removed and filtered using a 0.2-μm syringe microfilter (Millex-LG). Injections (10 μL) were made onto a reverse phase column (C-18, 5 μm, 4.6 × 250 mm, Waters symmetry 300). The mobile phase (prepared in HPLC grade water) contained 0.1 M citric acid, 1 mM hexyl sodium sulfate, 0.1 mm EDTA, and 10% methanol (pH 3.5) at a flow rate of 1 mL/min. Catecholamines were detected with a thin-layer radial electrochemical cell (BASi, West Lafayette, IN, USA) at a potential of 700 mV versus a Ag/AgCl reference electrode. Catecholamine standards were prepared from 10 mM stock solutions in 0.1 N $HClO_4$. A Labview stripchart recorder program (Jorgenson Lab, UNC-CH) was used for data collection through home built electronic equipment. The peak area of the analyte was ratioed to the peak area of the internal standard, HQ. After correction for differential detector response, the amount of analyte in the brain tissue was calculated.

Lidocaine microinfusion

Lidocaine was administered *via* an infusion cannula (33 gauge) that was combined with the bipolar stimulating electrodes and inserted into the implanted guide cannula (26 gauge, Plastics One Inc., VA, USA). Microinfusions (0.5 μL) were made over 60 s with a syringe pump (Kent Scientific Corporation, CT, USA). The regions targeted were normally the noradrenergic pathways, DNB and VNB. In one set of experiments, the noradrenergic cell bodies in the LC (AP -9.8 mm, ML +1.4 mm, DV 6.5-7.5 mm) and the NTS (AP -12.0 mm, ML +1.8 mm, DV 7.6-8.6 mm) were targeted.

Histology

At the end of experiments, electrode placements were verified by stereotaxically lowering a tungsten electrode to the original position of the carbon-fiber microelectrode. A lesion was made at the recording site by applying continuous current (20 μA for 10 s) to the tungsten electrode. Some lesions (> 20 rats) of the *v*BNST and the AV were made directly with the carbon-fiber microelectrodes, but this precluded postcalibration of the electrode sensitivity. These experiments verified the accuracy of the repositioning of tungsten electrodes in recording sites. Brains were removed from the skull, stored in 10 % formaldehyde for at least 3 days, and coronally sectioned into 40 μm slices with a cryostat. The sections were mounted on slides, stained with 0.2 % thionin, and coverslipped before viewing under a light microscope.

Drugs and reagents

All chemicals and drugs were reagent-quality or better and were used without additional purification. Drugs were obtained from Sigma-Aldrich (St. Louis, MO, USA) unless otherwise indicated. *In vitro* postcalibration of carbon-fiber microelectrodes was performed in a Tris buffer solution at a pH 7.4 containing 15 mM Tris, 140 mM NaCl, 3.25 mM KCl, 1.2 mM $CaCl_2$, 1.25 mM NaH_2PO_4, 1.2 mM $MgCl_2$, and 2.0 mM Na_2SO_4 in double distilled water (Mega Pure System, Corning Glasswork, Corning, NY). Lidocaine (100 μg/0.5 μL) was dissolved in saline and sterile filtered with the pH adjusted to 6 with NaOH. Desipramine-HCl, raclopride-HCl, clonidine-HCl and yohimbine-HCl were dissolved in saline. GBR 12909-HCl was dissolved in double distilled water and then diluted with saline. Injected volumes were 0.6 ml/kg and were given intraperitoneally (i.p.).

Data analysis

Clampfit 8.1 as part of pCLAMP 8.1 software package (Axon Instruments, Foster City, CA) was used to analyze half-life and signal amplitude values according to procedures described in the literature (Park *et al.* 2005). The half life of catecholamine uptake, $t_{1/2}$, was taken as

the time to descend from its maximum value to half of that value. Since uptake follows Michaelis-Menten kinetics, this procedure is an oversimplification. Nevertheless, we used it to obtain figures that give an approximate measure of the changes in data induced by the various drugs. Data are represented as mean ± S.E.M. and '*n*' values indicating the number of rats. Mean values were compared by using the two-tailed Student's *t*-test (GraphPad Software version 4.0, San Diego, CA, USA) to calculate the level of significance. $P < 0.05$ was regarded as statistically significant.

Results

Monoamine content of the *v*BNST

Two regions of *v*BNST were dissected from fresh brains and their monoamine (norepinephrine, dopamine and serotonin) content determined by HPLC (Table 1). The ratio of norepinephrine to dopamine content for the anteromedial *v*BNST (AP +0.5 to 0.0 mm from bregma) was ca. 2 to 1 whereas in the medioposterior *v*BNST region (AP 0.0 to -0.5 mm from bregma) it was ca. 10 to 1 consistent with a previous report (Kilts & Anderson, 1986). Serotonin was not detected in either subregion. The norepinephrine content in the medioposterior *v*BNST (3.25 ± 1.89 μg/g of tissue) is similar to the 2.1 μg/g of tissue previously found in the AV (Mitchell *et al.*, 1994), a region that also contains negligible dopamine (Oke *et al.*, 1983). The relatively large standard deviation for the neurochemical values in the *v*BNST is atypical of liquid chromatographic measurements and may well reflect the heterogeneity of this region and our failure to dissect exactly the same nuclei each time (the site in the *v*BNST that supports norepinephrine release is ~300 μm thick). However, the norepinephrine content in both of these regions is considerably less than the content of dopamine (9 μg/g of tissue) in the CPu, a region that contains little norepinephrine (Garris & Wightman, 1994).

Catecholamine overflow in the *v*BNST and AV as a function of stimulating electrode depth

In the first set of *in vivo* experiments, the carbon-fiber microelectrode was placed in the *v*BNST or AV while the stimulating electrode was lowered from 3.5 mm below the skull surface. Based on catecholamine content of *v*BNST, we lowered the carbon-fiber microelectrode in the medioposterior *v*BNST to monitor extracellular norepinephrine as shown in supplementary Figure 2.

Catecholamine overflow was monitored while the electrical stimulation was delivered at different depths. Stimulations (60 Hz, 60 pulses) were delivered at 200-300 μm intervals. Figure 1A shows the coronal plane (AP -5.2 mm) and track (dotted lines, centered on 1.2 mm ML) of the tips of the bipolar stimulating electrode. The DNB is located ~2 mm above the VTA/SN while the VNB passes within the VTA/SN (Ungerstedt, 1971; Miyahara & Oomura, 1982; Saphier, 1993). The maximum current in the cyclic voltammograms at the potential where catecholamines are oxidized (0.6 V vs Ag/AgCl) was recorded and plotted as a function of the position of the stimulating electrode (Figure 1B).

When the carbon-fiber microelectrode was in the *v*BNST responses were not observed until the stimulating electrode was below a depth of 5 mm. Evoked release reached an initial maximum at depths of 5.5-7.0 mm, the location of the DNB (Figure 1B) and a second maximal release was evoked between 8.2 and 8.8 mm beneath the skull surface, the location of the VNB. When at the level of the VNB, the stimulating electrode tips are in close proximity to the VTA/SN. Indeed, the dopamine cell bodies are also activated with VNB stimulation since catecholamine release was evoked in the CPu, a region containing little norepinephrine. DNB stimulation does not evoke catecholamine release in the CPu (Garris *et al.*, 1993). When the carbon-fiber microelectrode was in the AV, maximal release was

also observed with the stimulating electrode in the DNB (between 5.5 and 7.0 mm). However, catecholamine release in the AV was not detected when the stimulating electrode was at the level of the VNB. Individual traces and background-subtracted cyclic voltammograms recorded in the *v*BNST and AV along with their respective cyclic voltammograms are shown in Figure 1C.

The cyclic voltammograms recorded in different terminal regions are compared to authentic dopamine and norepinephrine in Figure 2. Although slight differences exist, within experimental error dopamine and norepinephrine cannot be distinguished based on their voltammograms. However, the cyclic voltammograms for the catecholamines are distinct from those for all other substances establishing that the evoked release is a catecholamine (Heien *et al.*, 2003). The signal for norepinephrine at a specific concentration is only 60 % of that for dopamine because it adsorbs to the electrode to a lesser extent (Heien *et al.*, 2004).

Spatial distribution of evoked norepinephrine by stimulation of the DNB or VNB

In the next series of experiments the stimulating electrode was fixed at a location in the DNB or the VNB while the carbon-fiber microelectrode was lowered through terminal regions. Figure 3A shows the coronal plane (AP 0.0 mm) that was used for investigating catecholamine release along a track that includes the *v*BNST. The carbon-fiber microelectrode was lowered from 4.2 to 8.5 mm below the skull surface (track shown by a dotted line in Figure 3A (left), 1.2 mm ML), and cyclic voltammograms were recorded at different vertical positions during electrical stimulations (60 Hz, 60 pulses). When the VNB was stimulated, catecholamine release was seen in two regions of the BNST as the carbon-fiber microelectrode was lowered (Figure 3A, right). Catecholamine overflow was maximal at ~6.0 mm, the level of the dorsal BNST (*d*BNST), disappeared at the level of the anterior commissure, and then reached a maximal response at ~7.3 mm, the level of the *v*BNST. When the stimulating electrode was in the DNB, only low release was evoked in the *d*BNST, none was seen at the level of the anterior commissure, and catecholamine release was maximal at the level of the *v*BNST (Figure 3A right). The responses in the *v*BNST were lower with the carbon fiber further posterior (AP - 0.4 to - 0.7 mm, data not shown), consistent with previous work (Forray & Gysling, 2004).

Figure 3B shows the coronal section containing the AV (AP -2.2 mm) in which the carbon-fiber microelectrode was lowered (ML 1.5 mm) from 4.2 to 7.2 mm from the skull surface while stimulated release was evoked as described above. The AV is at 4.9 to 5.7 mm along this tract. When the stimulating electrode was placed in the DNB, maximal catecholamine release was observed at 5.5 mm below the skull surface, coincident with the AV (Figure 3B, right). No release was seen below 6.2 mm. When the stimulating electrode was in the VNB, there was no detectable signal in the AV with the exception of a small signal in one out of six rats. This result is consistent with previous studies that catecholamine input into the AV is primarily through the DNB (Kobayashi *et al.*, 1974; Brun *et al.*, 1993).

Effect of autoreceptor antagonists and uptake blockers on catecholamine overflow in the AV and the CPu

To confirm the origin of the signals in the AV, we tested the effects of drugs known to act at noradrenergic neurons and compared their responses to drugs with known actions at dopaminergic neurons. α2-adrenoceptors down-regulate norepinephrine release, a process that is blocked by the antagonist yohimbine (Ghasemzadeh *et al.*, 1993). D2 receptors play a similar role on dopamine neurons where they act as autoreceptors and inhibit release. Thus, raclopride, a D2 antagonist, increases stimulated release from dopamine neurons (Seeman & Van Tol, 1993), but does not affect release from norepinephrine neurons (Gobert *et al.*,

1998). Desipramine selectively inhibits the norepinephrine transporter (NET), reducing the clearance rate of norepinephrine (Dugast *et al.*, 2002), but it does not affect the dopamine transporter (DAT) (Kula *et al.*, 1999). In contrast, GBR12909 blocks the DAT while it has no affect on the NET (Palij & Stamford, 1992; Dugast *et al.*, 2002).

The effects of noradrenergic drugs on stimulated release were evaluated in the AV (60 pulses, 60 Hz) and compared to dopaminergic responses in the CPu (24 pulses at 60 Hz, representative examples in Figure 4). Before drug administration the clearance half-life ($t_{1/2}$, the time required for the concentration to decay to 50 % of the maximum) in the AV was 1.28 ± 0.11 s (n = 15) in close agreement with that reported previously (Mitchell *et al.*, 1994). The half-life for catecholamine in the CPu was 0.83 ± 0.05 sec (n = 7) was almost half of that in the AV (t = 2.70, d.f. = 20, $P = 0.01$). Overflow in the AV was significantly increased 30 min after yohimbine (5 mg/kg). These changes were quantified by recording the maximal evoked release $[CA]_{max}$ and $t_{1/2}$. These are reported as a percent of predrug values in Table 2. Both parameters significantly increased after yohimbine in the AV. Injection of desipramine (15 mg/kg) 30 min after yohimbine further increased $[CA]_{max}$ and $t_{1/2}$. The effects of the drugs were apparent within 10 min of administration and reached a maximum value at ~30 min. Desipramine (15 mg/kg) alone, also significantly increased both $[CA]_{max}$ and $t_{1/2}$ in the AV. Note that the noradrenergic drugs at the same doses did not significantly change dopamine overflow in the CPu elicited by VTA/SN stimulations (Figure 4A, right, Table 2).

When dopaminergic drugs were applied, changes in stimulated release were only observed in the CPu with VTA/SN stimulation, but not in the AV with DNB stimulation (Table 2). The evoked response in the AV was not significantly changed by raclopride (2 mg/kg) or GBR 12909 (15 mg/kg)(Figure 4B, left). This work is consistent with prior results showing that electrically stimulated release in the AV is sensitive to drugs specific for the noradrenergic system but insensitive to drugs that affect dopaminergic neurons (Stamford *et al.*, 1988;Brun *et al.*, 1993). In contrast, both $[CA]_{max}$ and $t_{1/2}$ in the CPu were significantly increased after the raclopride (Figure 4B, right). Administration of GBR 12909, 30 min after raclopride, dramatically increased stimulated catecholamine overflow in the CPu. Evoked catecholamine overflow during control experiments with saline injection was stable and reproducible for at least 2 h (data not shown).

Pharmacological characterization of catecholamine overflow in the *v*BNST

While evoked release in the *v*BNST has been pharmacologically characterized in brain slices (Palij & Stamford, 1992; 1993), it has not *in vivo*. Therefore, evoked catecholamine release in the *v*BNST was also evaluated with noradrenergic specific (yohimbine, desipramine and the norepinephrine α2-adrenoceptor agonist, clonidine) and dopamine specific (raclopride and GBR 12909) drugs using both DNB and VNB stimulations (60 Hz, 60 pulses). Before drug administration, norepinephrine clearance in the *v*BNST had $t_{1/2}$ of 2.45 ± 0.19 sec (n = 8) for VNB and 2.19 ± 0.16 sec (n = 9) for DNB stimulations, values that are not significantly different from each other but that are significantly greater than in the AV (t = 5.73, d.f. = 21, $P < 0.0001$ for VNB and t = 4.83, d.f. = 22, $P < 0.0001$ for DNB). The half lives for catecholamine clearance before drugs in the *v*BNST with stimulation of either noradrenergic pathway were almost 3 times longer than in the CPu (t = 7.74, d.f. = 13, $P < 0.0001$ for VNB and t = 7.23, d.f. = 14, $P < 0.0001$ for DNB). Evoked release was significantly decreased 30 min after clonidine injection (0.2 mg/kg) with either DNB or VNB stimulations, a decrease that was reversed by yohimbine administration (5.0 mg/kg, Figure 5A). When yohimbine was administered alone, evoked release was significantly increased 30 min later (Figure 5B) with stimulations of both pathways. These responses were further increased with injection of desipramine 30 min later. The average results from all animals (Table 2) show that both $[CA]_{max}$ and $t_{1/2}$ were significantly increased by the

noradrenergic drugs. However, the effects of desipramine and yohimbine on $[CA]_{max}$ and $t_{1/2}$ in the *v*BNST were significantly less than in the AV (Table 2). Catecholamine overflow evoked by DNB or VNB stimulation in the *v*BNST was not changed by raclopride (2 mg/kg) or GBR 12909 (15 mg/kg, Figure 5C, Table 2).

After the experiments with yohimbine and desipramine in the *v*BNST, catecholamine overflow evoked by the stimulation of the DNB and the VNB was recorded for 20 min at 5 min intervals and, then, lidocaine (350 nmol) was microinfused onto the electrical stimulation tips. Lidocaine is a voltage-gated Na^+ channel blocker that prevents action potential generation (Boehnke & Rasmusson, 2001). It eliminated stimulated release within 5 min after its microinfusion (Figure 6) and stimulated release was partially restored 30 min later. Identical results were obtained when the stimulating electrode and microinfusion were placed in the noradrenergic cell bodies, either the LC or the NTS. Thus, catecholamine overflow in the *v*BNST is due to the neuronal responses originating from both the NTS and the LC.

Effects of the stimulation conditions on catecholamine overflow

The responses in each noradrenergic region to different stimulation parameters were investigated. Figure 7A shows that the amplitude increased in the AV and the *v*BNST with increasing stimulation frequency (10, 20, 40, and 60 Hz, 60 pulses). The evoked concentration change during a 20 Hz stimulation in the AV approached a plateau while the concentration change in the *v*BNST continued to increase during the stimulation. However, at higher frequencies in both regions the concentration increased during the stimulation. Figure 7B shows the responses in the *v*BNST and the AV with different pulse numbers (10, 20, 40 and 80 and 120 pulses at 60 Hz). Measurable responses (signal to noise (S/N) ≥ 5) were normally observed with at least 10 pulses at 60 Hz with our present instrumentation. The extracellular catecholamine concentration evoked by both DNB and VNB stimulation in the *v*BNST increased with pulse number but the stimulated release in the AV did not increase when more than 40 pulses were used. Pooled maximal responses are shown in Figure 7C and D. The maximum evoked catecholamine concentration ($[CA]_{max}$) at 60 Hz, 40 pulses in the CPu with stimulation at the level of the VNB was ~11 times greater than in the *v*BNST and AV in Table 3.

Discussion

This study provides novel neurochemical information for two brain regions, the AV and vBNST, that receive high densities of noradrenergic input. The AV receives major input from the hippocampal formation via the mammillary bodies of the hypothalamus and has reciprocal connections with limbic circuits. While the functional significance of norepinephrine signaling in the AV has not been extensively studied, it is thought to play an important role in behavioral learning and memory and the conscious perception of emotion (Gabriel *et al.*, 1980; Sparenborg & Gabriel, 1992; Oda *et al.*, 2003). Conversely, the BNST is highly connected to the ventral subiculum of the hippocampus, neocortex, the paraventricular and supraoptic nucleus of the hypothalamus, the ventral tegmental area and other limbic structures such as the amygdala (Dong & Swanson, 2004; Forray & Gysling, 2004; Massi *et al.*, 2008). The norepinephrine input to *v*BNST plays a key role in stress and drug related behaviors (Delfs *et al.*, 2000; Fendt *et al.*, 2005). However, investigation of noradrenergic transmission within the AV and *v*BNST is extremely difficult because of the small size of these nuclei. The present study provides a foundation for studies of norepinephrine communication in animal behaviors such as learning and fear in these brain regions. The results clearly show that norepinephrine neurotransmission has regionally specific characteristics in discrete regions of the brain that can be monitored with carbon-fiber microelectrodes and fast-scan cyclic voltammetry. The select positioning of stimulating

electrodes in either noradrenergic pathways (Figure 1) or cell body regions (Figure 6) allows characterization of noradrenergic afferents that innervate small brain regions such as the AV and *v*BNST.

These two regions were selected for this initial study because their norepinephrine content is high relative to dopamine. Moreover, measurements in brain slices have shown that norepinephrine release in the *v*BNST can be evoked with local stimulation and have identified the pharmacological control points in these regions (Palij & Stamford, 1992; 1993; Miles *et al.*, 2002). Our brain mapping and pharmacological investigations in the intact animal expand upon that work. A major finding is that the noradrenergic inputs into the *v*BNST from both the DNB and VNB provide have quite similar capacity for release. We also found that control by autoreceptors and NET is quite similar for the neurons of both pathways into the *v*BNST. In contrast, the regulation of release and uptake was strikingly different in the AV, a region only innervated by the DNB.

Evidence that the monitored signal in the *v*BNST and the AV is a catecholamine

The background-subtracted cyclic voltammograms provide a “fingerprint” that identifies the released substance(s) as a catecholamine (Figure 2). These cyclic voltammograms enable the catecholamines to be distinguished from other substances such as serotonin, ascorbic acid, and catecholamine metabolites (Palij & Stamford, 1992;Heien *et al.*, 2003). Another approach that has been used to monitor norepinephrine is differential pulse amperometry (Suaud-Chagny *et al.*, 1990;Brun *et al.*, 1993). This method can resolve catecholamines from ascorbate but not from their metabolites and suffers from a slow response time. Continuous amperometry has also been used (Dugast *et al.*, 2002;Yavich *et al.*, 2005). This approach has little chemical selectivity but can be used to establish that the half-life of evoked norepinephrine and dopamine is on the time scale of seconds.

Unfortunately, like all other electrochemical techniques, background-subtracted cyclic voltammograms cannot distinguish between norepinephrine and dopamine although the cyclic voltammograms enable the catecholamines to be distinguished from the other substances as mentioned above. Epinephrine also has similar electrochemical properties to dopamine and norepinephrine but the epinephrine tissue content is sufficiently low in the brain regions investigated that it is unlikely to be measured (Van der Gugten *et al.*, 1976; Kilts & Anderson, 1986). Our assignment of the evoked signals measured in the AV and *v*BNST to norepinephrine thus relies heavily on the neurochemical results (Table 1) that show that dopamine is a minority catecholamine in each region (Oke *et al.*, 1983; Kilts & Anderson, 1986; Mitchell *et al.*, 1994). Furthermore, immunofluorescence and autoradiographic tracing have shown that the AV and the *v*BNST receive few dopaminergic terminals (Segal *et al.*, 1973; Swanson & Hartman, 1975; Versteeg *et al.*, 1976; Freedman & Cassell, 1994; Kozicz, 2001). However, we are hesitant to assign the species detected in regions where the tissue content of dopamine and norepinephrine is similar or has not been established even when the cyclic voltammograms have the characteristic shape of a catecholamine. For example, release seen in the *d*BNST with VNB stimulation (Figure 3A), a region that contains similar amounts of dopamine and norepinephrine (Kilts & Anderson, 1986), likely contains a dopamine component because the VNB stimulation also excites dopamine cell bodies in the VTA/SN.

Mapping inputs to the AV and *v*BNST

The small size of the carbon-fiber microelectrode enables maps to be generated of sites that support catecholamine release with up to 100 μm resolution, and enable *in vivo* tracking of neuronal pathways. While such maps have been generated previously for dopamine pathways (Garris *et al.*, 1994; Garris & Wightman, 1994), their use to explore

norepinephrine (Suaud-Chagny *et al.*, 1986) innervation is less extensive. When the carbon-fiber microelectrode was implanted either within the *v*BNST or the AV, electrical stimulation of the DNB, the pathway of the noradrenergic neurons from the LC and other nuclei (Kobayashi *et al.*, 1974; Moore & Bloom, 1979), evoked catecholamine release in both brain regions (Figure 3). Prior work has shown that this stimulation location does not support release in the CPu (Garris *et al.*, 1993). When the stimulating electrode was lowered to the VNB, robust catecholamine release was observed in the *v*BNST, but no release was observed in the AV. This is consistent with the lack of VNB noradrenergic projections to the AV (Moore & Card, 1984). The VNB stimulation also evoked release in the CPu because the cell bodies for dopamine, the predominant catecholamine in this region, are in the VTA/SN which is also stimulated at the coordinates we used for the VNB. Thus, the absence of a response in the AV also confirms that it lacks dopaminergic inputs.

The VNB noradrenergic input into the *v*BNST has been demonstrated by retrograde labeling (Terenzi & Ingram, 1995; Delfs *et al.*, 2000; Forray *et al.*, 2000). This assignment is supported by our pharmacological, voltammetric, and neurochemical measurements that show that the catecholamine detected is norepinephrine and not dopamine even though we were directly activating dopamine neurons with the site we selected for VNB stimulation. More surprising is the robust norepinephrine release obtained with DNB stimulation. These findings are consistent with anatomical evidence of a projection to the *v*BNST from the LC (Lindvall & Stenevi, 1978; McNaughton & Mason, 1980) *via* the DNB (Moore, 1978; Phelix *et al.*, 1992), a concept suggested by Adams and coworkers (Mitchell *et al.*, 1994). In support of the dual noradrenergic inputs to the *v*BNST, norepinephrine release was evoked by both the direct stimulation of the LC and the NTS (Figure 6), the origins of the two pathways. Despite similar amounts available for release in the *v*BNST from the two pathways, it appears that they are activated by different conditions during animal behaviors. For example, during opiate withdrawal, the noradrenergic neurons of the VNB are stimulated to a greater degree than those of the DNB (Delfs *et al.*, 2000)

Comparison of stimulated norepinephrine release in the AV and *v*BNST

The various stimulation parameters and pharmacological agents that we employed revealed significant differences in the characteristics of release and uptake in these two norepinephrine rich regions. The rapid time resolution of the recordings at carbon-fiber microelectrodes enabled the dynamics of release and uptake to be characterized with subsecond temporal resolution, revealing these differences. The pharmacological studies reveal that release and uptake in both regions is affected by noradrenergic drugs providing additional evidence that the observed release is norepinephrine. Furthermore, release in both regions is unaffected by dopaminergic drugs at doses that are highly effective in the modulation of dopamine release in the striatum. Indeed, the high selectivity of the drugs used in this work for the dopaminergic and noradrenergic pathways indicates that they can be used to distinguish dopamine and norepinephrine release as long as autoreceptors and the NET or DAT are exerting exclusive control on extracellular catecholamine levels.

The half-life measurements for norepinephrine disappearance after evoked release suggest that uptake is approximately twice as fast in the AV as in the *v*BNST. The sensitivity of the clearance to desipramine in both regions, coupled with their insensitivity to GBR 12909, clearly shows that clearance is due to uptake mediated by NET. While the absolute values of $t_{1/2}$ given in the Results section are not corrected for the response time of the electrode, they do show similar trends to those reported previously with continuous amperometry. In accord with our findings, norepinephrine uptake in the AV was reported to be significantly slower than for dopamine uptake in the striatum (Dugast *et al.*, 1994; Dugast *et al.*, 2002). Slower uptake allows extrasynaptic neurotransmitters to participate in volume transmission because they can diffuse greater distances before removal from the extracellular fluid by the

transporter. Interestingly, the measured half-life for clearance measured in the *v*BNST was independent of the noradrenergic pathway stimulated. Thus, it appears that the same uptake sites are controlling uptake, irrespective of the pathway from which release originates.

The inhibition of the α2-adrenoceptor increased release evoked by VNB stimulation in the *v*BNST and by DNB stimulation in both the AV and *v*BNST. However, the increase in release was significantly greater in the AV than with stimulation of either pathway innervating the *v*BNST (Table 2), indicating stronger control by noradrenergic autoreceptors in the AV. Thus, release and uptake by autoreceptors and NET are both more tightly regulated in the AV compared to the *v*BNST.

In addition to the greater control of extracellular norepinephrine in the AV evidenced by pharmacological studies, there are notable differences in the release evoked in each region. DNB stimulation causes similar amounts of release in each region (Table 3). Furthermore, VNB stimulation, which does not evoke release in the AV, causes release of a similar concentration in the *v*BNST. In the *v*BNST the frequency dependence of release is quite similar to that reported in dopamine regions (Garris & Wightman, 1994). During low frequency stimulations (10-20 Hz), which are in the physiological range, norepinephrine concentrations approach a new, steady-state level during the stimulation (Figure 7). This behavior is that expected for neurotransmitter systems in which extracellular levels are maintained by the balance between uptake and release. At higher frequencies release takes more pulses to overwhelm uptake, and evoked concentrations continue to rise during the stimulation in the *v*BNST. However, in the AV, the stronger uptake coupled with the greater inhibition by autoreceptors, results in a greater control of norepinephrine concentrations during long stimulations leading to a lack of sensitivity to pulse number even with frequencies as high as 60 Hz stimulations (Figure 7). The importance of uptake control in the AV is clearly apparent with the dramatic increase in release amplitude following NET inhibition (Table 2). Thus, norepinephrine response in the AV resembles that at the rat tail artery where norepinephrine shows strong control by uptake (Msghina *et al.*, 1999), with additional control of extracellular levels by the noradrenergic autoreceptor.

Conclusion

In the present study, we showed that in *vivo* fast-scan cyclic voltammetry coupled with carbon-fiber microelectrodes enable monitoring of rapid changes in norepinephrine concentration in the *v*BNST and the AV of anesthetized rats despite the small size of these regions and the low amounts of norepinephrine compared to that of dopamine in the striatum. This study also demonstrates that norepinephrine release in the *v*BNST was evoked by the stimulation of either DNB or VNB whereas only DNB stimulation evoked norepinephrine release in the AV. In both regions, released norepinephrine was regulated by autoreceptors and restored to prestimulus levels by uptake. However, control by autoreceptors and uptake was much stronger in the AV than in the *v*BNST.

Supplementary Material

Refer to Web version on PubMed Central for supplementary material.

Acknowledgments

We thank Andy Seipel, Leslie Sombers and Brandon Aragona for providing technical assistance. The authors are also indebted to Khristy Fontillas, Brandon Aragona and Nii Addy for helpful comments regarding the manuscript. This work was supported by NIH (NS 15841).

References

Aston-Jones G, Cohen JD. An integrative theory of locus coeruleus-norepinephrine function: adaptive gain and optimal performance. Annu Rev Neurosci. 2005; 28:403–450. [PubMed: 16022602]

Berridge CW, Waterhouse BD. The locus coeruleus-noradrenergic system: modulation of behavioral state and state-dependent cognitive processes. Brain Res Brain Res Rev. 2003; 42:33–84. [PubMed: 12668290]

Boehnke SE, Rasmusson DD. Time course and effective spread of lidocaine and tetrodotoxin delivered via microdialysis: an electrophysiological study in cerebral cortex. J Neurosci Methods. 2001; 105:133–141. [PubMed: 11275270]

Brun P, Suaud-Chagny MF, Gonon F, Buda M. In vivo noradrenaline release evoked in the anteroventral thalamic nucleus by locus ceruleus activation: an electrochemical study. Neuroscience. 1993; 52:961–972. [PubMed: 8095714]

Cahill PS, Wightman RM. Simultaneous amperometric measurement of ascorbate and catecholamine secretion from individual bovine adrenal medullary cells. Anal Chem. 1995; 67:2599–2605. [PubMed: 8849026]

Delfs JM, Zhu Y, Druhan JP, Aston-Jones G. Noradrenaline in the ventral forebrain is critical for opiate withdrawal-induced aversion. Nature. 2000; 403:430–434. [PubMed: 10667795]

Dong HW, Swanson LW. Organization of axonal projections from the anterolateral area of the bed nuclei of the stria terminalis. J Comp Neurol. 2004; 468:277–298. [PubMed: 14648685]

Dugast C, Cespuglio R, Suaud-Chagny MF. In vivo monitoring of evoked noradrenaline release in the rat anteroventral thalamic nucleus by continuous amperometry. J Neurochem. 2002; 82:529–537. [PubMed: 12153477]

Dugast C, Suaud-Chagny MF, Gonon F. Continuous in vivo monitoring of evoked dopamine release in the rat nucleus accumbens by amperometry. Neuroscience. 1994; 62:647–654. [PubMed: 7870296]

Fendt M, Siegl S, Steiniger-Brach B. Noradrenaline transmission within the ventral bed nucleus of the stria terminalis is critical for fear behavior induced by trimethylthiazoline, a component of fox odor. J Neurosci. 2005; 25:5998–6004. [PubMed: 15976089]

Forray MI, Gysling K. Role of noradrenergic projections to the bed nucleus of the stria terminalis in the regulation of the hypothalamic-pituitary-adrenal axis. Brain Res Brain Res Rev. 2004; 47:145–160. [PubMed: 15572169]

Forray MI, Gysling K, Andres ME, Bustos G, Araneda S. Medullary noradrenergic neurons projecting to the bed nucleus of the stria terminalis express mRNA for the NMDA-NR1 receptor. Brain Res Bull. 2000; 52:163–169. [PubMed: 10822157]

Freedman LJ, Cassell MD. Distribution of dopaminergic fibers in the central division of the extended amygdala of the rat. Brain Res. 1994; 633:243–252. [PubMed: 7511034]

Gabriel M, Foster K, Orona E. Interaction of laminae of the cingulate cortex with the anteroventral thalamus during behavioral learning. Science. 1980; 208:1050–1052. [PubMed: 7375917]

Garris PA, Ciolkowski EL, Wightman RM. Heterogeneity of evoked dopamine overflow within the striatal and striatoamygdaloid regions. Neuroscience. 1994; 59:417–427. [PubMed: 8008199]

Garris PA, Collins LB, Jones SR, Wightman RM. Evoked extracellular dopamine in vivo in the medial prefrontal cortex. J Neurochem. 1993; 61:637–647. [PubMed: 8336146]

Garris PA, Wightman RM. Different kinetics govern dopaminergic transmission in the amygdala, prefrontal cortex, and striatum: an in vivo voltammetric study. J Neurosci. 1994; 14:442–450. [PubMed: 8283249]

Ghasemzadeh MB, Capella P, Mitchell K, Adams RN. Real-time monitoring of electrically stimulated norepinephrine release in rat thalamus: I. Resolution of transmitter and metabolite signal components. J Neurochem. 1993; 60:442–448. [PubMed: 8419530]

Gobert A, Rivet JM, Audinot V, Newman-Tancredi A, Cistarelli L, Millan MJ. Simultaneous quantification of serotonin, dopamine and noradrenaline levels in single frontal cortex dialysates of freely-moving rats reveals a complex pattern of reciprocal auto- and heteroreceptor-mediated control of release. Neuroscience. 1998; 84:413–429. [PubMed: 9539213]

Heien ML, Johnson MA, Wightman RM. Resolving neurotransmitters detected by fast-scan cyclic voltammetry. Anal Chem. 2004; 76:5697–5704. [PubMed: 15456288]

Heien ML, Phillips PE, Stuber GD, Seipel AT, Wightman RM. Overoxidation of carbon-fiber microelectrodes enhances dopamine adsorption and increases sensitivity. Analyst. 2003; 128:1413–1419. [PubMed: 14737224]

Johnston CA, Mattiace LA, Negro-Vilar A. Effect of ventral noradrenergic bundle lesions on concentrations of monoamine neurotransmitters and metabolites in several discrete areas of the rat brain. Cell Mol Neurobiol. 1987; 7:403–411. [PubMed: 2454160]

Kilts CD, Anderson CM. The simultaneous quantification of dopamine, norepinephrine and epinephrine in micropunched rat brain nuclei by on-line trace enrichment HPLC with electrochemical detection: Distribution of catecholamines in the limbic system. Neurochem Int. 1986; 9:437–445. [PubMed: 20493144]

Kobayashi RM, Palkovits M, Kopin IJ, Jacobowitz DM. Biochemical mapping of noradrenergic nerves arising from the rat locus coeruleus. Brain Res. 1974; 77:269–279. [PubMed: 4152793]

Kozicz T. Axon terminals containing tyrosine hydroxylase- and dopamine-beta-hydroxylase immunoreactivity form synapses with galanin immunoreactive neurons in the lateral division of the bed nucleus of the stria terminalis in the rat. Brain Res. 2001; 914:23–33. [PubMed: 11578594]

Kula NS, Baldessarini RJ, Tarazi FI, Fisser R, Wang S, Trometer J, Neumeyer JL. [3H]beta-CIT: a radioligand for dopamine transporters in rat brain tissue. Eur J Pharmacol. 1999; 385:291–294. [PubMed: 10607889]

Lindvall O, Stenevi U. Dopamine and noradrenaline neurons projecting to the septal area in the rat. Cell Tissue Res. 1978; 190:383–407. [PubMed: 688339]

Massi L, Elezgarai I, Puente N, Reguero L, Grandes P, Manzoni OJ, Georges F. Cannabinoid receptors in the bed nucleus of the stria terminalis control cortical excitation of midbrain dopamine cells in vivo. J Neurosci. 2008; 28:10496–10508. [PubMed: 18923026]

McNaughton N, Mason ST. The neuropsychology and neuropharmacology of the dorsal ascending noradrenergic bundle--a review. Prog Neurobiol. 1980; 14:157–219. [PubMed: 6999536]

Miles PR, Mundorf ML, Wightman RM. Release and uptake of catecholamines in the bed nucleus of the stria terminalis measured in the mouse brain slice. Synapse. 2002; 44:188–197. [PubMed: 11954051]

Millar J, Stamford JA, Kruk ZL, Wightman RM. Electrochemical, pharmacological and electrophysiological evidence of rapid dopamine release and removal in the rat caudate nucleus following electrical stimulation of the median forebrain bundle. Eur J Pharmacol. 1985; 109:341–348. [PubMed: 3872803]

Mitchell K, Oke AF, Adams RN. In vivo dynamics of norepinephrine release-reuptake in multiple terminal field regions of rat brain. J Neurochem. 1994; 63:917–926. [PubMed: 8051568]

Miyahara S, Oomura Y. Inhibitory action of the ventral noradrenergic bundle on the lateral hypothalamic neurons through alpha-noradrenergic mechanisms in the rat. Brain Res. 1982; 234:459–463. [PubMed: 6277435]

Moore RY. Catecholamin innervation of the basal forebrain. I. The septal area. J Comp Neurol. 1978; 177:665–684. [PubMed: 75215]

Moore RY, Bloom FE. Central catecholamine neuron systems: anatomy and physiology of the norepinephrine and epinephrine systems. Annu Rev Neurosci. 1979; 2:113–168. [PubMed: 231924]

Moore, RY.; Card, JP. Noradrenaline-containing neuron systems. In: Bjorklund, A.; Hokfelt, T., editors. Handbook of Chemical Neruoanatomy: Classical Neurotransmitters in the CNS, Part I. Elsevier; Amsterdam: 1984.

Msghina M, Gonon F, Stjärne L. Facilitation and depression of ATP and noradrenaline release from sympathetic nerves of rat tail artery. J Physiol (Lond). 1999; 515:523–531. [PubMed: 10050018]

Oda S, Kuroda M, Kakuta S, Tanihata S, Ishikawa Y, Kishi K. Ultrastructure of ascending cholinergic terminals in the anteroventral thalamic nucleus of the rat: a comparison with the mammillothalamic terminals. Brain Res Bull. 2003; 59:473–483. [PubMed: 12576145]

Oke A, Solnick J, Adams RN. Catecholamine distribution patterns in rat thalamus. Brain Res. 1983; 269:180–183. [PubMed: 6871698]

Onaka T, Yagi K. Role of noradrenergic projections to the bed nucleus of the stria terminalis in neuroendocrine and behavioral responses to fear-related stimuli in rats. Brain Res. 1998; 788:287–293. [PubMed: 9555060]

Owesson-White CA, Cheer JF, Beyene M, Carelli RM, Wightman RM. Dynamic changes in accumbens dopamine correlate with learning during intracranial self-stimulation. Proc Natl Acad Sci U S A. 2008; 105:11957–11962. [PubMed: 18689678]

Palij P, Stamford JA. Real-time monitoring of endogenous noradrenaline release in rat brain slices using fast cyclic voltammetry: 1. Characterisation of evoked noradrenaline efflux and uptake from nerve terminals in the bed nucleus of stria terminalis, pars ventralis. Brain Res. 1992; 587:137–146. [PubMed: 1525644]

Palij P, Stamford JA. Real-time monitoring of endogenous noradrenaline release in rat brain slices using fast cyclic voltammetry. 2. Operational characteristics of the alpha 2 autoreceptor in the bed nucleus of stria terminalis, pars ventralis. Brain Res. 1993; 607:134–140. [PubMed: 8097660]

Paxinos, G. The Rat Nervous System. 2nd. Academic Press; San Diego: 1995.

Paxinos, G.; Watson, C. The Rat Brain in Stereotaxic Coordinates. Elsevier Inc.; Burlington: 2007.

Phelix CF, Liposits Z, Paull WK. Monoamine innervation of bed nucleus of stria terminalis: an electron microscopic investigation. Brain Res Bull. 1992; 28:949–965. [PubMed: 1379113]

Saphier D. Electrophysiology and neuropharmacology of noradrenergic projections to rat PVN magnocellular neurons. Am J Physiol. 1993; 264:R891–902. [PubMed: 8388662]

Seeman P, Van Tol HH. Dopamine receptor pharmacology. Curr Opin Neurol Neurosurg. 1993; 6:602–608. [PubMed: 8104554]

Segal M, Pickel V, Bloom F. The projections of the nucleus locus coeruleus: an autoradiographic study. Life Sci. 1973; 13:817–821. [PubMed: 4766258]

Sparenborg S, Gabriel M. Local norepinephrine depletion and learning-related neuronal activity in cingulate cortex and anterior thalamus of rabbits. Exp Brain Res. 1992; 92:267–285. [PubMed: 1493864]

Stamford JA, Kruk ZL, Millar J. Stimulated limbic and striatal dopamine release measured by fast cyclic voltammetry: anatomical, electrochemical and pharmacological characterisation. Brain Res. 1988; 454:282–288. [PubMed: 3261616]

Suaud-Chagny MF, Mermet C, Gonon F. Electrically evoked noradrenaline release in the rat hypothalamic paraventricular nucleus studied by in vivo electrochemistry: characterization and facilitation by increasing the stimulation frequency. Neuroscience. 1990; 34:411–422. [PubMed: 2333151]

Suaud-Chagny MF, Steinberg R, Mermet C, Biziere K, Gonon F. In vivo voltammetric monitoring of catecholamine metabolism in the A1 and A2 regions of the rat medulla oblongata. J Neurochem. 1986; 47:1141–1147. [PubMed: 3091764]

Swanson LW, Hartman BK. The central adrenergic system. An immunofluorescence study of the location of cell bodies and their efferent connections in the rat utilizing dopamine-beta-hydroxylase as a marker. J Comp Neurol. 1975; 163:467–505. [PubMed: 1100685]

Terenzi MG, Ingram CD. A combined immunocytochemical and retrograde tracing study of noradrenergic connections between the caudal medulla and bed nuclei of the stria terminalis. Brain Res. 1995; 672:289–297. [PubMed: 7749750]

Ungerstedt U. Stereotaxic mapping of the monoamine pathways in the rat brain. Acta Physiol Scand Suppl. 1971; 367:1–48. [PubMed: 4109331]

Van der Gugten J, Palkovits M, Wijnen HL, Versteeg DH. Regional distribution of adrenaline in rat brain. Brain Res. 1976; 107:171–175. [PubMed: 1268720]

Van Groen T, Kadish I, Michael Wyss J. Role of the anterodorsal and anteroventral nuclei of the thalamus in spatial memory in the rat. Behav Brain Res. 2002; 132:19–28. [PubMed: 11853854]

Versteeg DH, Van Der Gugten J, De Jong W, Palkovits M. Regional concentrations of noradrenaline and dopamine in rat brain. Brain Res. 1976; 113:563–574. [PubMed: 953752]

Yavich L, Jakala P, Tanila H. Noradrenaline overflow in mouse dentate gyrus following locus coeruleus and natural stimulation: real-time monitoring by in vivo voltammetry. J Neurochem. 2005; 95:641–650. [PubMed: 16248883]

Abbreviations

***v*BNST**	ventral bed nucleus of the stria terminalis
AV	anteroventral thalamic nucleus
DNB	dorsal noradrenergic bundle
VNB	ventral noradrenergic bundle
VTA/SN	ventral tegmental area/substantia nigra
NET	norepinephrine transporter
DAT	dopamine transporter
LC	the locus coeruleus
NTS	nucleus tractus solitarius
CPu	cadate-putamen

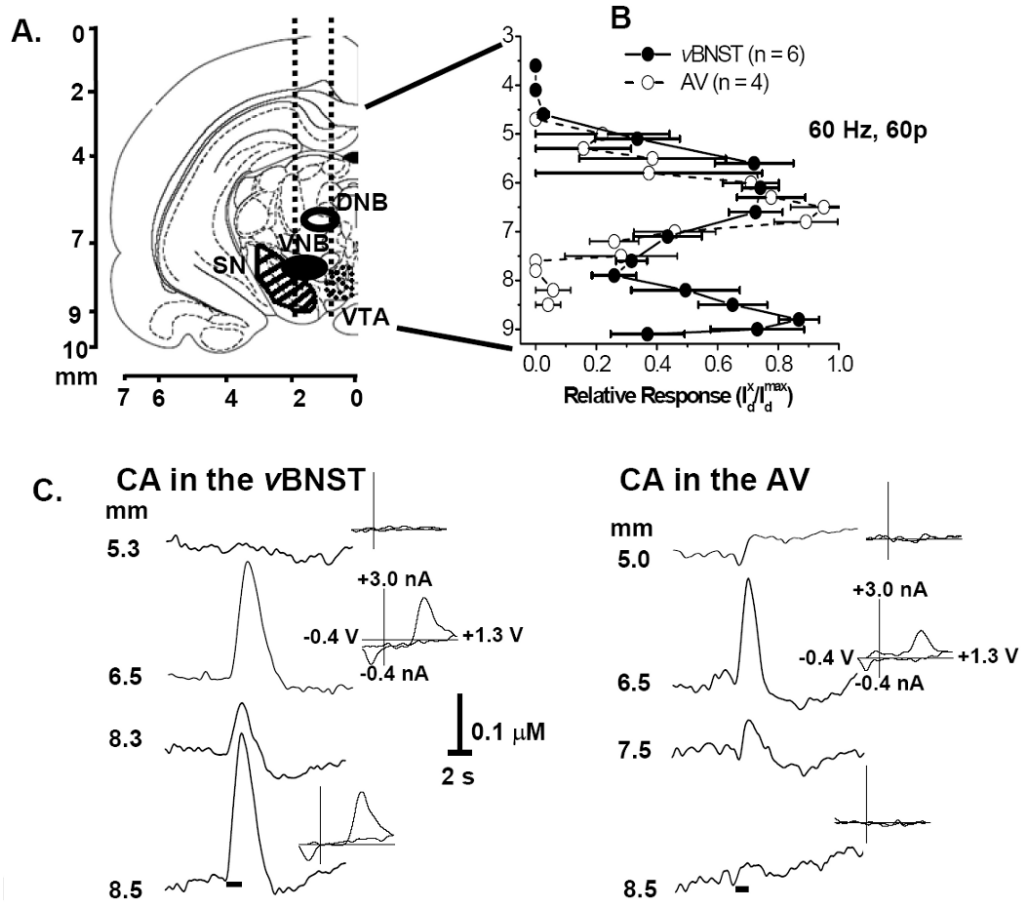

Figure 1.

Maps of maximal stimulated release of catecholamines measured in the AV and the *v*BNST as a function of depth of the stimulating electrode. A. The dotted lines show the approximate track of each of the two poles of the stimulating electrode. They are superimposed on a coronal section containing the DNB and into the VTA/SN and VNB. Abbreviations used: DNB, dorsal noradrenergic bundle; VNB, ventral noradrenergic bundle; VTA, ventral tegmental area; SN, substantia nigra. The coronal section is from the atlas of Paxinos and Watson (2007). B. Maximal stimulated release during electrical stimulations (60 Hz, 60 pulses) measured in the *v*BNST (—) and the AV (---) as the stimulating electrode was lowered in small increments through the regions shown in (A). The relative response is the response at a particular depth (I_d^x) divided by the maximum response (I_d^{max}). Note that the distance scale is different in panels A and B. C. Representative individual responses at the peak current for catecholamines in the BNST (left) and the AV (right) measured at the depth indicated in mm. The bars under the current traces denote the period of electrical stimulation. Insets: Background-subtracted cyclic voltammograms measured during the evoked responses. The concentration bars are based on postcalibration in norepinephrine solutions.

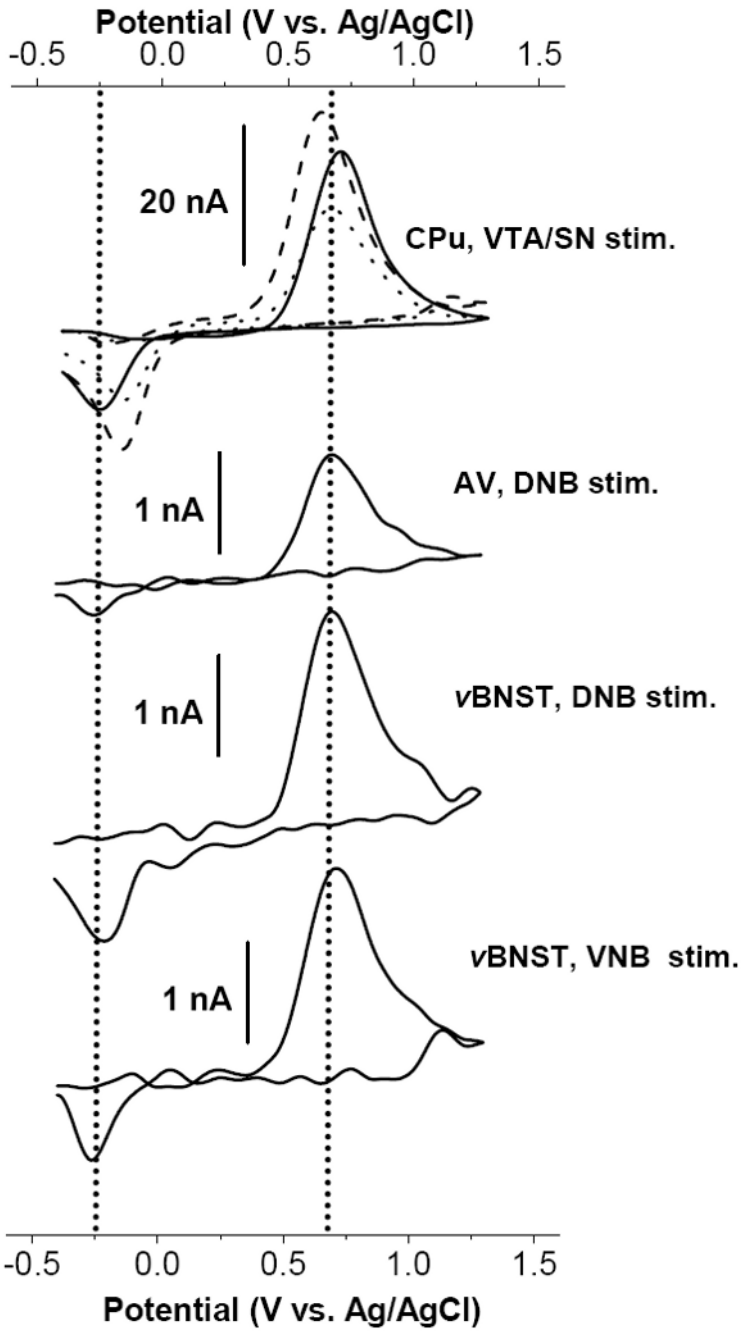

Figure 2.

Background-subtracted cyclic voltammograms measured in the BNST, the AV and the CPu at the end of DNB or VTA/SN and VNB stimulations (60 Hz, 60 pulses). In the upper trace, cyclic voltammograms are also shown for authentic norepinephrine (⋯) and dopamine (---, both at 4 μM) in a Tris buffer solution at a pH 7.4 recorded after *in vivo* measurement.

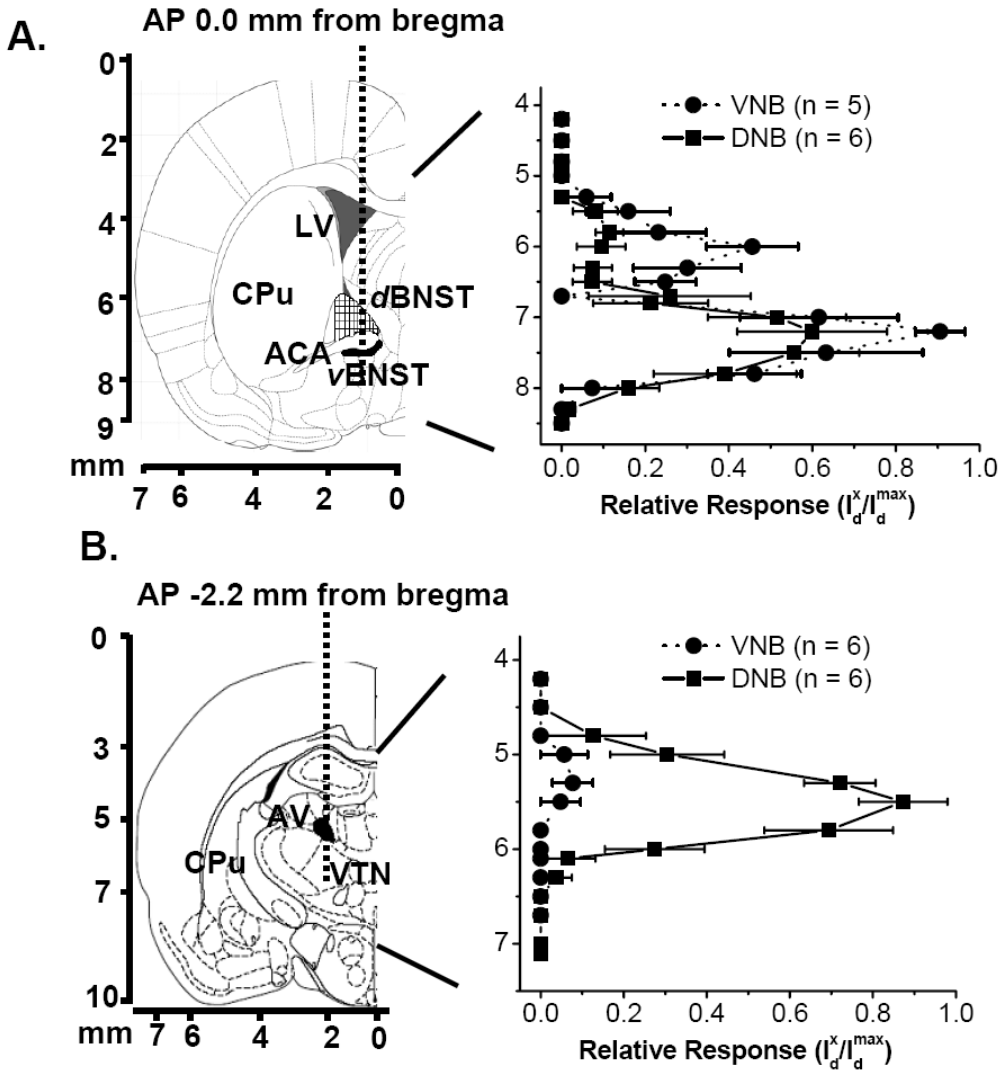

Figure 3.

Maps of stimulated norepinephrine release within the AV and BNST with stimulation of the VNB and DNB. A. The dotted line in the coronal section (AP 0.0 mm from bregma) illustrate the approximate path of the carbon-fiber microelectrodes in the BNST aimed at the dorsal (*d*, hatched area above the ACA) and ventral (*v*, filled region below the ACA) BNST. The right part of the figure shows maximal evoked responses detected in the cyclic voltammograms following electrical stimulation (60 Hz, 60 pulses) of the VNB (···) or the DNB (—). Data are normalized as in Figure 1. B. The dotted line in the coronal section (AP -2.2 mm from bregma) shows the approximate path of the carbon-fiber microelectrodes in the AV (filled region). The right part of the figure shows maximal evoked responses from the cyclic voltammograms recorded after electrical stimulation (60 Hz, 60 pulses) of the VNB (···) or the DNB (—). Data normalized as in Figure 1. The coronal sections were taken from the atlas of Paxinos and Watson (2007). Abbreviations used: ACA, anterior commissure; CPu, caudate-putamen; LV, lateral ventricle; VTN, ventral thalamic nucleus.

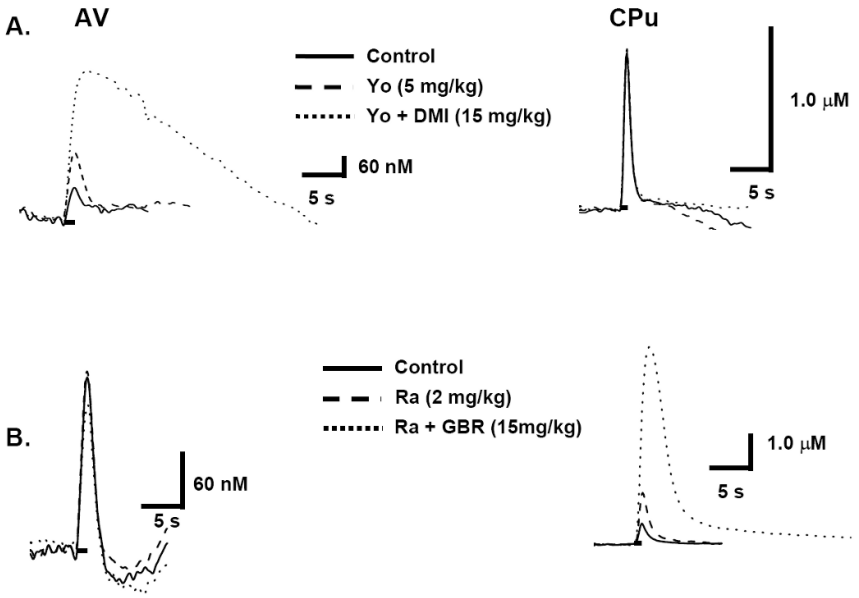

Figure 4.

Effect of yohimbine (Yo, 5 mg/kg), desipramine (DMI, 15 mg/kg), raclopride (Ra, 2 mg/kg) and GBR 12909 (GBR, 15 mg/kg) on catecholamine overflow in the AV and the CPu. A. Recordings of extracellular catecholamine in the AV (left) evoked by DNB stimulation with 60 pulses and in the CPu (right) evoked by VTA/SN stimulation with 24 pulses in the absence and presence of Yo (---) and Yo + DMI (⋯) at 60 Hz. B. Recordings of extracellular catecholamine in the AV (left) evoked by the DNB stimulation with 60 pulses and in the CPu (right) evoked by VTA/SN stimulation with 24 pulses in the absence and presence of Ra (---) and Ra + GBR (⋯) at 60 Hz. The bars under the current traces indicate the period of electrical stimulation.

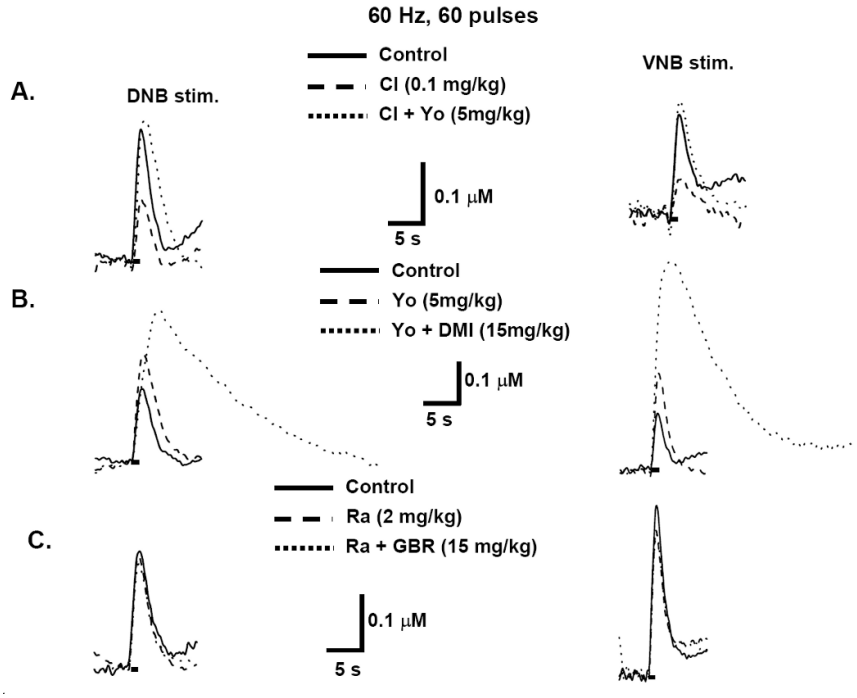

Figure 5.

Effect of clonidine (Cl, 0.2 mg/kg), yohimbine (Yo, 5 mg/kg), desipramine (DMI, 15 mg/kg), raclopride (Ra, 2 mg/kg) and GBR 12909 (GBR, 15 mg/kg) on catecholamine overflow in the *v*BNST. Representative recordings of extracellular catecholamine in the *v*BNST evoked by DNB stimulation (left) or VNB stimulation (right) in the absence and presence of (A) Cl (---) and Cl + Yo (⋯), (B) Yo (---) and Yo + DMI (⋯) and (C) Ra (---) and Ra + GBR 12909 (⋯) at 60 Hz with 60 pulses. The bars under the current traces indicate the period of electrical stimulation.

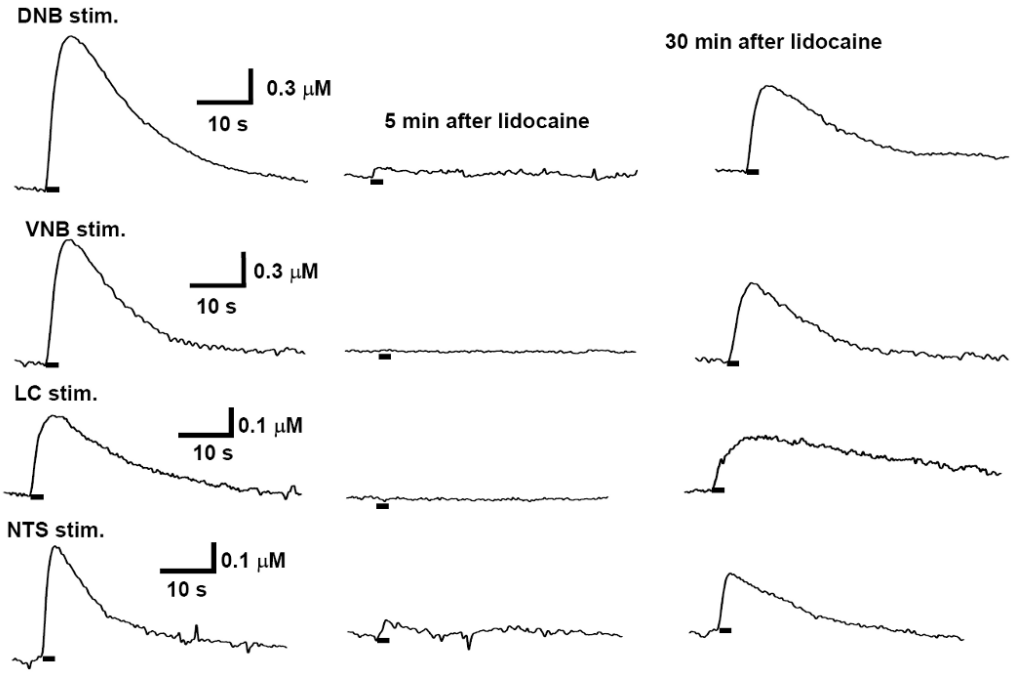

Figure 6.

Effect of lidocaine on catecholamine response in the *v*BNST after drug study (Yo + DMI). Catecholamine response in the *v*BNST before (left), 5 min after (middle) and 30 min after (right) lidocaine (350 nmol/min) infused into the sites of the electrical stimulation (DNB, VNB, LC and NTS – one site per animal). An infusion cannula was combined with the bipolar stimulating electrodes. Abbreviations used: DNB, dorsal noradrenergic bundle; VNB, ventral noradrenergic bundle; LC, locus coeruleus; NTS, nucleus tractus solitarius. The bars under the current traces indicate the period of electrical stimulation.

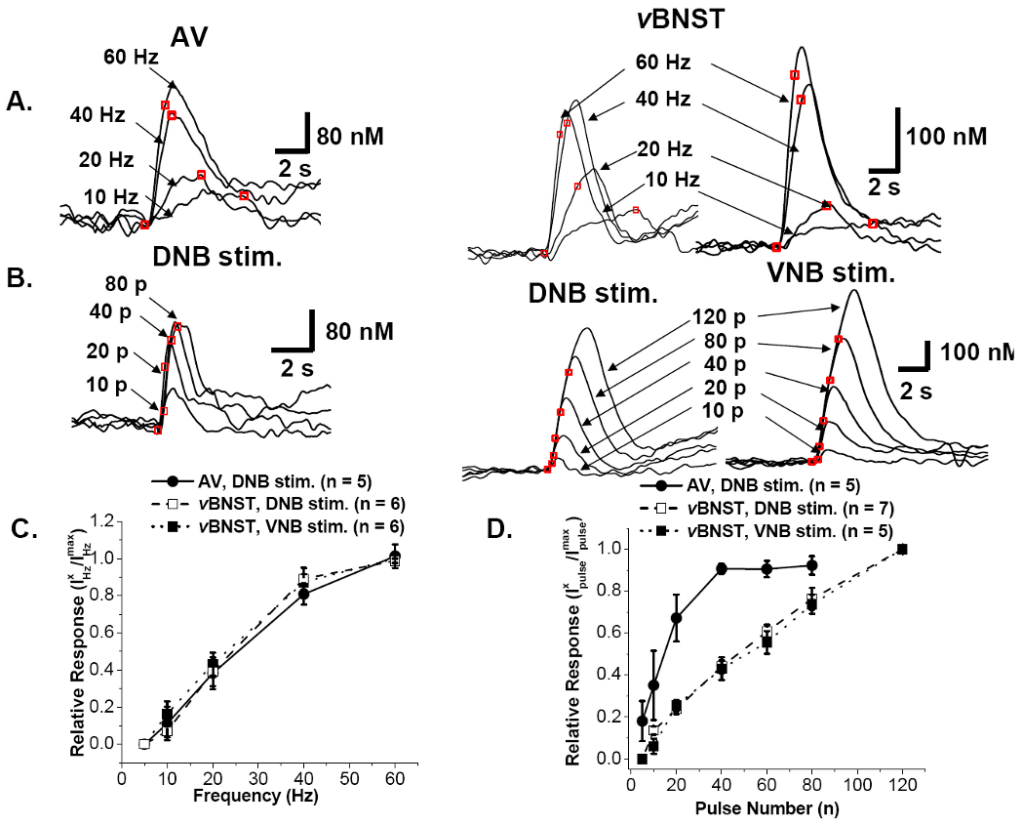

Figure 7.

Effect of frequency and pulse number (stimulus duration) on catecholamine overflow. A. Individual catecholamine overflows in the AV (left) evoked by DNB stimulation and in the *v*BNST evoked by DNB and VNB stimulation (right) for pulse frequency (10, 20, 40 and 60 Hz) with 60 pulses. B. Effect of pulse number (10, 20, 40, 80 and 120 for *v*BNST) on catecholamine in the AV (left) and in the *v*BNST (right) is shown. Initiation and termination of stimuli were indicated by the boxes. C. Maximal catecholamine responses in the AV and the *v*BNST as a function of stimulation frequency. D. Maximal catecholamine responses in the AV and *v*BNST as a function of pulse number. Relative responses in C and D are the monitored response (I^x) divided by the maximum response (I^{max}).

Table 1

Monoamine content in the *v*BNST. Values represent the mean ± S.E.M.

***v*BNST**	**AnteroMedial (µg/g, n = 12 trials)**	**MedioPosterior (µg/g, n = 12 trials)**
Norepinephrine	2.01 ± 0.75*	3.25 ± 1.89*
Dopamine	1.18 ± 0.25	0.34 ± 0.29 #
Serotonin	n.d.	n.d.

* Indicates significantly different from dopamine ($P < 0.05$) in the MedioPosterior.

Significantly different from dopamine in the AnteroMedial *v*BNST (t = 2.2, d.f. = 22, $P = 0.04$). n.d. : not detectable.

Table 2

Effects of yohimbine (Yo, 5 mg/kg), desipramine (DMI, 15 mg/kg), raclopride (Ra, 2 mg/kg) and GBR 12909 (GBR,15 mg/kg) with raclopride on the time course of catecholamine overflow.

Drug (n ≥ 4)		**(%) of control**			
	Brain Region	**AV**	**CPu**	***v*BNST**	
	Stimulation	**DNB**	**VNB**	**DNB**	**VNB**
Yo	$[CA]_{max}$	247 ± 21*&	101 ± 6	154 ± 10*	188 ± 11*
	$t_{1/2}$	169 ± 10*	106 ± 7	132 ± 12*	143 ± 9*
Yo + DMI	$[CA]_{max}$	630 ± 45*#&	93 ± 2	223 ± 15*#	286 ± 31 *#
	$t_{1/2}$	1065 ± 17*#&	101 ± 2	463 ± 65 *#	455 ± 48*#
DMI	$[CA]_{max}$	302 ± 16*&	-	172 ± 21*	157 ± 9*
	$t_{1/2}$	1423 ± 197*&	-	505 ± 90*	330 ± 34*
Ra	$[CA]_{max}$	98 ± 4	311 ± 27*	92 ± 4	96 ± 2
	$t_{1/2}$	106 ± 5	129 ± 12	99 ± 4	110 ± 5
Ra + GBR	$[CA]_{max}$	104 ± 7	736 ± 106 *#	90 ± 5	89 ± 4
	$t_{1/2}$	105 ± 3	285 ± 51 *#	104 ± 4	105 ± 5

Data are mean ± S.E.M. and were obtained during 60 Hz stimulations (60 pulses for the AV and *v*BNST and 24 pulses for the CPu). The maximal catecholamine concentration, $[CA]_{max}$, and the time required for catecholamine overflow decay to 50 % of the maximum, $t_{1/2}$, are shown.

*Indicates significantly different from control values ($P < 0.05$).

#Significantly different from yohimbine or raclopride values ($P < 0.05$).

&Significantly different from *v*BNST values ($P < 0.01$).

Table 3

$[CA]_{max}$ in the *v*BNST, the AV and the CPu evoked by the electrical stimulation (60 Hz, 40 pulses). Values represent the mean ± S.E.M. (n ≥ 7).

	AV	*v*BNST		CPu
Stimulation site	**DNB**	**VNB**	**DNB**	**VNB**
$[CA]_{max}$ μM	0.13 ± 0.02	0.15 ± 0.01	0.17 ± 0.02	1.85 ± 0.32*

$[CA]_{max}$ is maximum extracellular catecholamine concentration.

*Indicates significant difference of $[CA]_{max}$ evoked by the electrical stimulation in the CPu from that in the *v*BNST (t = 5.2, d.f. = 12, $P = 0.0002$) and the AV (t = 5.7, d.f. = 13, $P < 0.0001$).